

DOI: 10.1002/cctc.201300378

# Facile Synthesis of a Nanocrystalline Metal–Organic Framework Impregnated with a Phosphovanadomolybdate and Its Remarkable Catalytic Performance in Ultradeep Oxidative Desulfurization

Yiwei Liu,<sup>[a]</sup> Shumei Liu,<sup>[a]</sup> Shuxia Liu,<sup>\*[a]</sup> Dadong Liang,<sup>[a]</sup> Shujun Li,<sup>[a]</sup> Qun Tang,<sup>[a]</sup> Xingquan Wang,<sup>[a]</sup> Jun Miao,<sup>[a]</sup> Zhan Shi,<sup>[b]</sup> and Zhiping Zheng<sup>\*[c, d]</sup>

Reducing the level of sulfur content in fuel oils has long been desired for environmental reasons. Polyoxometalates (POMs) can act as catalysts to remove sulfur-containing heterocyclic compounds by the process of oxidative desulfurization under mild conditions. However, one key obstacle to the development of POM-based catalysts is the poor solubility of POMs in the overall nonpolar environment. We report a novel strategy for the introduction of catalytically active POMs into nonpolar reaction systems by encapsulating the inorganic catalyst

within the pores of a metal–organic framework structure in which the organic ligands act as hydrophobic groups. The nanocrystalline catalysts, obtained rapidly and conveniently by both solution and mechanochemical synthesis, showed remarkable activities in catalytic oxidative desulfurization reactions in both a model diesel environment and in real diesel wherein dibenzothiophene was converted rapidly and quantitatively into dibenzothiophene sulfone.

## Introduction

Sulfur oxides resulting from burning fuel oils are responsible for smog, acid rain, and respiratory problems in human beings. Thus, reducing the level of sulfur content is not only necessary but also important. At present, the main approach to decrease sulfur levels is hydrodesulfurization (HDS).<sup>[1]</sup> There are two problems inherently associated with this process. One problem is the high costs associated with the demanding reaction conditions, such as high reaction temperature and the consumption of high-pressure hydrogen gas. The second problem is

that this approach is efficient in removing thiols, sulfides, and disulfides but not as effective in removing sulfur-containing heterocyclic compounds, in particular dibenzothiophene (DBT) and its derivatives. Therefore, developing non-HDS methods have been long desired.<sup>[2]</sup>

Oxidative desulfurization (ODS) is an alternative strategy in which the refractory organosulfur compounds are oxidized into the corresponding sulfones; these sulfones are subsequently removed by extraction. This process relies on an oxidant, commonly H<sub>2</sub>O<sub>2</sub>, together with a catalyst, often an ionic liquid<sup>[3]</sup> or a heteropolyacid.<sup>[4]</sup> Given that large-scale use of peroxides is dangerous, molecular oxygen would be a preferred oxidant. Equally desirable is the use of environmentally benign catalysts, a representative is polyoxometalates (POMs).<sup>[5]</sup> Despite great efforts made and significant progress achieved, one key obstacle to the development of POM-based catalysts is the poor solubility of POMs in overall nonpolar environments.<sup>[6]</sup> One solution is the use of amphiphilic POMs for which the metal–oxo cores are charge compensated with cationic surfactants; solubilization and stabilization are achieved by the formation of an emulsion, which results from hydrophobic interactions between the surfactant and the nonpolar medium.<sup>[7]</sup> Unfortunately, in addition to their cumbersome preparation, emulsions are inherently metastable; breakdown of the system results in POM leaching and phase separation from the reaction medium, and this leads to compromised catalytic performance.


Recognizing the challenge of engaging the organic substrates with the inorganic catalysts, we recently set out to design a novel class of materials featuring catalytically active

[a] Y. Liu, Dr. S. Liu, Prof. Dr. S. Liu, Dr. D. Liang, S. Li, Q. Tang, X. Wang, J. Miao  
Key Laboratory of Polyoxometalate Science of the Ministry of Education  
Faculty of Chemistry  
Northeast Normal University  
Ren Min Street No.5268, Changchun, Jilin 130024 (China)  
Fax: (+86)431-85099328  
E-mail: liusx@nenu.edu.cn

[b] Dr. Z. Shi  
State Key Laboratory of Inorganic Synthesis and Preparative Chemistry  
College of Chemistry  
Jilin University  
Changchun, Jilin 130012 (China)

[c] Prof. Dr. Z. Zheng  
Frontier Institute of Science and Technology  
Xi'an Jiaotong University  
Xi'an, Shaanxi 710054 (China)

[d] Prof. Dr. Z. Zheng  
Department of Chemistry  
University of Arizona  
Tucson, Arizona 85721 (USA)  
E-mail: zhiping@email.arizona.edu

 Supporting information for this article is available on the WWW under <http://dx.doi.org/10.1002/cctc.201300378>.

POMs encased by highly porous metal–organic frameworks (MOFs),<sup>[8]</sup> denoted as POMs@MOFs. The primary consideration is the promotion of substrate–catalyst interactions in the confinement of the framework. We noticed that if the organic part of the MOFs was similar to the amphiphilic POM catalyst, the organic ligands in the MOFs could act as hydrophobic groups to introduce the POMs into the nonpolar medium and adsorb the organic substrates. As a result, our aim may be achieved by substrate diffusion into the porous structure and ideally in close proximity to the encapsulated catalyst. Accordingly, occupation of these pores by substrate molecules serves to pre-concentrate the reactants, which may possibly lead to enhanced reaction kinetics as a result of favorable and “intensified” substrate–catalyst organization. Furthermore, considering the aromatic nature of the targeted substrates, bridging ligands featuring aromatic fragment(s) should be utilized in the assembly of the MOF structure.

## Results and Discussion

We report herein the preparation and structural characterization of such a material and the remarkable catalytic performance of its nanocrystals for the oxidation of DBT. The compound, formulated as  $[(\text{CH}_3)_4\text{N}]_2[\text{Cu}_2(\text{BTC})_{4/3}(\text{H}_2\text{O})_2]_6^- [\text{H}_3\text{PV}_2\text{Mo}_{10}\text{O}_{40}] \cdot 14\text{H}_2\text{O}$  (NENU-9, BTC = 1,3,5-benzenetricarboxylate), was originally obtained under hydrothermal conditions starting from copper nitrate; 1,3,5-benzenetricarboxylic acid ( $\text{H}_3\text{BTC}$ );  $[(\text{CH}_3)_4\text{N}]\text{OH}$ ; and  $\text{H}_5\text{PV}_2\text{Mo}_{10}\text{O}_{40}$  (POVM), a phosphovanadomolybdate extensively studied for the ODS of thiophenes. Crystallographic studies revealed a structure constructed from paddle-wheel  $\text{Cu}_2$  units and bridging BTC ligands (Figure S1, Supporting Information), which is isostructural to previously reported NENU- $n$  ( $n=1-6$ ) in which three kinds of pores (types A, B, and C) were identified.<sup>[9]</sup> The most salient difference is that the POMs occupying the type A pores in the present structure are the catalytically active POVm.

It was quickly realized that the crystal material was not particularly useful for ODS because of the large particle size, which limits its dispersion in diesel fuels and which limits the uptake of DBT. Nanocrystals, owing to their unique behavior as a result of their reduced size, occupy a significant portion of the novel materials developed for different applications.<sup>[10]</sup> However, the preparation of POMs@MOFs nanocrystalline materials has been rarely taken into account. Recognizing the unique behavior of nanomaterials as a result of their reduced size and aiming to improve the catalytic performance of the materials in hand, we explored the preparation of  $[\text{Cu}_2(\text{BTC})_{4/3}(\text{H}_2\text{O})_2]_6^- [\text{H}_5\text{PV}_2\text{Mo}_{10}\text{O}_{40}]$  (NENU-9N), the nanocrystalline form of the original compound. We subsequently succeeded in the preparation of phase-pure NENU-9N under ambient conditions.

### Preparation of pure-phase nanocrystalline catalysts

In a typical preparation, the copper salt and an excess amount of POVm were dissolved in distilled water. The pH of the solution was adjusted to 2.5. Then, a solution of a stoichiometric amount of  $\text{H}_3\text{BTC}$  (relative to  $\text{Cu}^{2+}$ ) in ethanol was added. A

green precipitate was collected. The synthesis was finished within minutes. Considering that POMs are introduced into the frameworks as noncoordinated guests, the isostructural  $[\text{Cu}_3(\text{BTC})_2]$  framework without POMs could also be obtained under the same conditions. The phase purity was confirmed by powder X-ray diffraction (PXRD) studies. Through detailed comparison of the PXRD patterns of NENU-9 and  $[\text{Cu}_3(\text{BTC})_2]$ , a notable difference in the patterns was revealed, that is, the peak at  $2\theta=9.48^\circ$ , which can be identified as the characteristic peak of  $[\text{Cu}_3(\text{BTC})_2]$  but not of NENU-9. To obtain phase-pure NENU-9N, we systematically varied the concentration of POVm and found that the characteristic peak of  $[\text{Cu}_3(\text{BTC})_2]$  disappeared only if POVm was used in an excess amount, but all the other diffraction peaks could be readily indexed to NENU-9 (Figure 1). We concluded that although interactions between the  $\text{Cu}^{2+}$  cations and the POM anions exist,<sup>[11]</sup> if the amount of the POM added was not high enough, some of the  $\text{Cu}^{2+}$  cat-

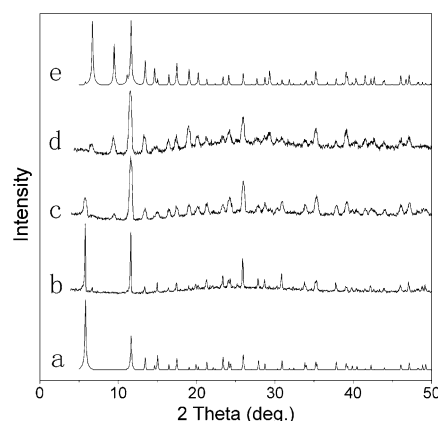


**Figure 1.** PXRD patterns of a) NENU-9 (simulated), b) products obtained with an excess amount of POVm, c) products obtained by using a stoichiometric ratio, d) products obtained with an insufficient amount of POVm, and e)  $[\text{Cu}_3(\text{BTC})_2]$  (simulated). The experimental details are listed in Table S2, Supporting Information.

ions coordinate with BTC to form  $[\text{Cu}_3(\text{BTC})_2]$  and the rest of the  $\text{Cu}^{2+}$  cations generate NENU-9N. As the concentration of the POM is increased, the  $\text{Cu}^{2+}$  cations cannot escape from the POM anions, which results in phase-pure NENU-9N. Interestingly, the color change of the products from blue (for  $[\text{Cu}_3(\text{BTC})_2]$ ) to green (for NENU-9) is consistent with an increase in purity, which provides convenient evidence to initially judge the purity of the product (Figure S2, Supporting Information).

Pure-phase NENU-9N can be more readily prepared by mechanochemical synthesis, but the nanocrystals are not well faceted (Figure S3, Supporting Information). The nanocrystals prepared by different methods can be readily dispersed in decalin (Figure S4, Supporting Information), which is the model solution for diesel fuels.

The nature of the copper salt and the pH of the solution have profound effects on the size of the nanocrystals. We observed that under otherwise identical conditions, the use of copper acetate caused instant precipitation, whereas the reaction mixture remained clear for a certain period of time if

other copper salts (nitrate, sulfate, and chloride) were used. These observations may be rationalized in terms of the structural similarity between the paddle-wheel  $\text{Cu}_2$  units of copper acetate and those of NENU-9N. As anticipated, faster reactions produced smaller particles, whereas slower reactions favored larger particles, and this is consistent with the results in Figure 2, which shows the samples obtained by using copper nitrate and copper acetate, respectively. Similar observations were made by Wöll and co-workers who studied the assembly mechanism of MOFs.<sup>[12]</sup>

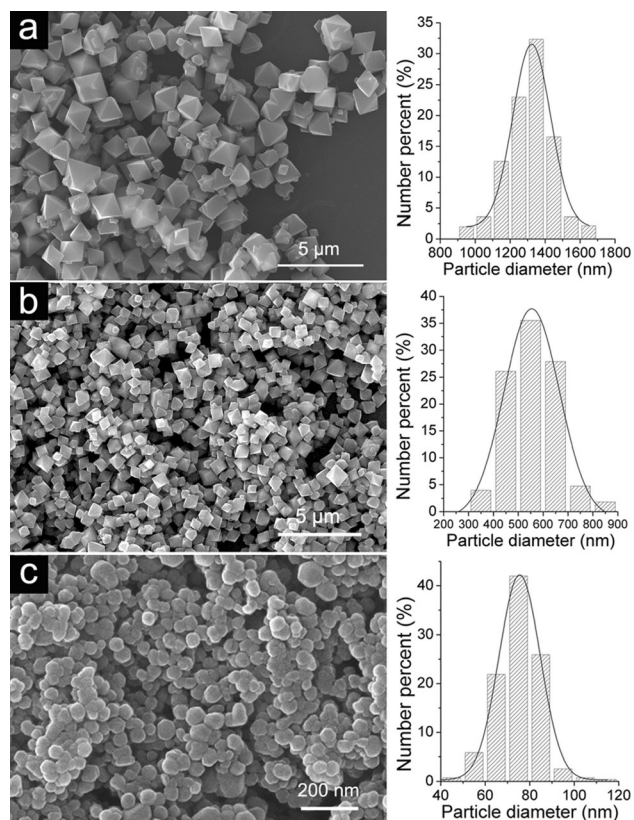


**Figure 2.** Field emission SEM of NENU-9N with a) copper nitrate as the metal source at pH 2.5, b) copper acetate as the metal source at pH 2.5, and c) copper acetate as the metal source at pH 4.0.

Considering the assembly process of NENU-9N, it is not surprising that pH is significant in controlling the reaction kinetics and, thus, the size of the resulting nanocrystals. Specifically, higher pH values favor the formation of BTC and its subsequent coordination with copper ions, and this leads putatively to smaller particles. Indeed, with the use of copper acetate at pH 2.5, nanocrystals were produced with an average size of 550 nm, whereas at pH 4.0, much smaller but less well-faceted nanocrystals were produced with an average size of 80 nm (Figure 2).

### Adsorption

As a necessary step in assessing the potential catalytic applications of NENU-9N, nitrogen adsorption experiments were per-

formed at 77 K by using both NENU-9 and NENU-9N. Type I sorption behavior was observed in both cases, and this suggests that the microporosity was preserved (Figure S5, Supporting Information). Notably, the BET specific surface area increased by 35% from 418 to 564  $\text{m}^2\text{g}^{-1}$  as the size was reduced, which is significant for an enhancement in the substrate adsorption and, ultimately, the catalytic performance. Applying Dubinin–Astakhov (DA) analysis to the isotherm data showed that the pore sizes were distributed narrowly at approximately 8.7 and 8.5 Å for NENU-9 and NENU-9N, respectively (Figure S6, Supporting Information)

How effectively DBT may be adsorbed into NENU-9N was then investigated. As a representative study, a mixture of NENU-9N and DBT in decalin was stirred continuously. The mixture was sampled periodically and analyzed by gas chromatography. The adsorption curve (Figure S7, Supporting Information) clearly demonstrates facile and efficient uptake of DBT. Complete adsorption was achieved within minutes, and this indicates efficient preconcentration and portends the great catalytic potential of NENU-9N. Such excellent adsorption properties are attributable thermodynamically to the favorable interactions between DBT and the hydrophobic environment provided by the type B pores<sup>[2c,d]</sup> and kinetically to the reduced size of the particles, which promotes facile diffusion of the substrates.<sup>[10c,13]</sup>

### Oxidative desulfurization

The catalytic activity of NENU-9N was investigated by the oxidation of DBT to dibenzothiophene sulfone ( $\text{DBTO}_2$ ) in decalin by using molecular oxygen as the oxidant. The reaction proceeded rapidly: approximately 90% of DBT was converted in approximately 60 min, and complete conversion was observed after an additional 30 min (Figure 3). FTIR suggested  $\text{DBTO}_2$  was the only product (Figure S8, Supporting Information). Comparative studies with the use of 300  $\mu\text{m}$  NENU-9 and POVM were performed. The conversion percentage after 90 min under otherwise identical conditions reached only approximately 41 and 2% for NENU-9 and POVM, respectively (Figure 3). Clearly, inorganic POVM cannot interact very well with DBT in the overall organic media. With the use of crystal-

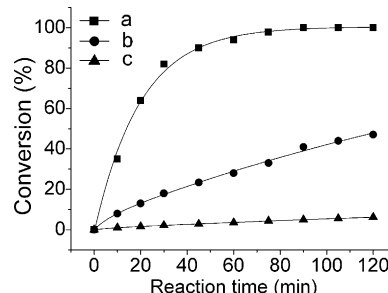


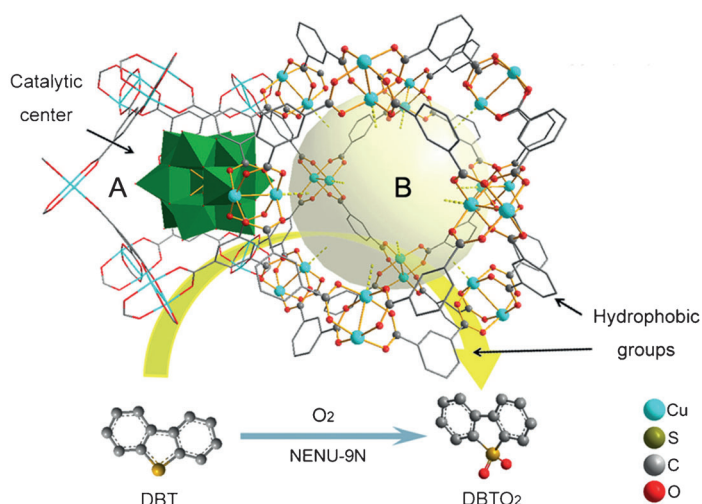
**Figure 3.** The percentage of DBT-to- $\text{DBTO}_2$  conversion versus reaction time by using a) NENU-9N (average diameter = 550 nm), b) NENU-9 (average diameter = 300  $\mu\text{m}$ ), and c) POVM (average diameter = 300  $\mu\text{m}$ ) as catalysts. Reaction conditions: catalyst (0.01 mmol), DBT (147 mg, 0.8 mmol), and isobutyraldehyde (0.72 mL, 8 mmol) in decalin (50 mL) at 80 °C.

line NENU-9 as the catalyst, although improved catalysis was observed as a result of MOF encapsulation of the POM, the reaction failed to achieve complete conversion even after an extended period of 120 min. These results unambiguously demonstrate the significance of housing POMs in an organic environment to promote substrate–catalyst interactions and also demonstrate the necessity to reduce the size of the catalyst-impregnated MOF to achieve stable dispersion for facile and maximized adsorption of the substrates and for enhanced kinetics of the catalytic reactions. The turnover frequency (TOF) was  $80 \text{ h}^{-1}$  for NENU-9N with an average diameter of 550 nm, which is higher than the previously reported TOF of other POVM-based catalysts in emulsion systems ( $\text{TOF} \approx 53 \text{ h}^{-1}$ ).<sup>[7c]</sup> In the catalytic process, aldehyde is needed, which is easily oxidized to the corresponding peracid that then oxidizes DBT to DBTO<sub>2</sub>.<sup>[14]</sup> The two steps are detailed in the Supporting Information.

Of great interest in developing green catalysts is the potential recovery of the catalyst by filtration or centrifugation. Both the structural integrity (Figure S9 and S10, Supporting Information) and the activity (Figure S11, Supporting Information) of the catalyst were maintained after the catalyst was reused over a number of cycles. We also performed a leaching test of fresh NENU-9N. The UV/Vis spectrum indicated that no POVM was leached even after the catalyst had been soaked for 48 h (Figure S12, Supporting Information).

The remarkable performance of the catalyst points to yet another great feature, that is, the MOF pores serve as nanostructured reactors that do not get clogged by the products. If the channels were blocked, the reaction would have become increasingly sluggish, and the catalyst would have been deactivated quickly. To rationalize these observations, one may consider the nature of the pores. They are hydrophobic and favor aromatic guests owing to the presence of a large number of benzene rings. It is thus reasonable to argue that occupancy by less polar and planar DBT is favored over occupancy by more polar and less planar DBTO<sub>2</sub>. This subtle difference in intermolecular interactions may be critical in keeping the flow of a continuous reaction: The highly polar sulfones vacate the pores for subsequent occupation by additional thiophene molecules. As such, the catalytic activity is maintained. Corroborating evidence is the deposition of a large amount of needlelike crystals (Figure S13, Supporting Information), identified as DBTO<sub>2</sub>, upon cooling of the reaction mixture to room temperature; highly polar DBTO<sub>2</sub> crystallized out from the much less polar decalin in essentially quantitative yield.

It is then possible to propose a mechanism for the oxidation of DBT to DBTO<sub>2</sub> catalyzed by NENU-9N (Scheme 1). Driven by hydrophobic–hydrophobic and aromatic–aromatic interactions with type B pores and facilitated by the reduced size of the catalyst and hence stable dispersion of the nanocrystals in solution, the DBT molecules are adsorbed and “forced” to interact with POVM, as they are confined in close proximity. DBTO<sub>2</sub>, the product, escapes through the channels.



**Scheme 1.** The possible catalytic process for the conversion of DBT into DBTO<sub>2</sub>. Two kinds of pores are marked (types A and B). Type A pores are occupied by POVM units.

With such excellent catalytic activity observed in model diesel, oxidation of prehydrotreated diesel was also performed to evaluate the catalytic capacity of NENU-9N in a real diesel environment. Only decalin was substituted by prehydrotreated diesel [sulfur content = 500 parts per million by weight (ppmw)], and otherwise the reaction conditions were identical. The conversion of DBT into DBTO<sub>2</sub> was complete in approximately 1.5 h, which is similar to the reaction in the model diesel environment. However, a difference was that there was no clear precipitation of the sulfones, but they could be further removed by a polar extractant.<sup>[4d,15]</sup> Ultradeep desulfurized diesel was thus obtained (Figure S14, Supporting Information).

## Conclusions

In summary, we report a novel strategy for the introduction of catalytically active POMs into nonpolar reaction systems by encapsulating the inorganic catalyst within the pores of a MOF structure. The nanocrystalline catalyst, which was obtained rapidly and conveniently by both solution and mechanochemical synthesis, showed remarkable activity in a catalytic oxidative desulfurization reaction, wherein DBT was converted rapidly and quantitatively into DBTO<sub>2</sub>. Effective preconcentration of the substrate molecules, made possible by the attractive forces between such molecules and the pore structures and as a result of the shortened diffusion path, is believed to be critical for the enhanced reactivity. This strategy should be readily extendable to the synthesis of other MOF-encapsulated POM catalysts, including those that are useful for liquid-phase catalytic reactions, especially in nonpolar media.

## Experimental Section

### Materials

All the raw chemicals were obtained commercially and used without additional purification. The H<sub>5</sub>PV<sub>2</sub>Mo<sub>10</sub>O<sub>40</sub>·34.5H<sub>2</sub>O precursor



was synthesized according to a procedure described in the literature and characterized by IR spectroscopy (Figure S15, Supporting Information).<sup>[16]</sup>

### Characterization

FTIR spectra were recorded in the 400–4000  $\text{cm}^{-1}$  range with an Alpha Centaur FTIR spectrophotometer by using KBr pellets. Thermogravimetric (TG) analyses were performed with a Perkin–Elmer TGA7 instrument in flowing  $\text{N}_2$  with a heating rate of  $10^\circ\text{C}\text{min}^{-1}$ . Powder X-ray diffraction (PXRD) measurements were performed with a Rigaku D/MAX-3 instrument with  $\text{CuK}_\alpha$  radiation in the  $2\theta = 3\text{--}50^\circ$  range at 293 K. A Hiden isochema IGA 100B instrument was used to measure  $\text{N}_2$  sorption. The progress of the catalytic reactions and liquid adsorption experiments were monitored by gas chromatography (Shimadzu GC-14C instrument). Morphology analysis of the POM nanocrystalline materials was performed by using a Quanta 250 FEG scanning electron microscope. UV/Vis spectra were recorded with a UV-6100 Double Beam spectrophotometer.

Single-crystal diffraction was conducted with a Bruker Smart Apex CCD diffractometer with  $\text{MoK}_\alpha$  monochromated radiation ( $\lambda = 0.71073 \text{ \AA}$ ) at room temperature. The linear absorption coefficients, scattering factors for the atoms, and anomalous dispersion corrections were taken from the International Tables for X-ray Crystallography. Empirical absorption corrections were applied. The structures were solved by using the direct method and refined through the full-matrix least-squares method on  $F^2$  by using SHELXS-97. Anisotropic thermal parameters were used to refine all non-hydrogen atoms, except for crystallization water oxygen and  $(\text{CH}_3)_4\text{N}^+$  cations. The hydrogen atoms attached to carbon positions were placed in geometrically calculated positions. Approximately 26 water molecules were estimated by TG analyses (Figure S18, Supporting Information), and only partial oxygen atoms of water molecules were achieved with the X-ray structure analysis. The crystal data and structure refinement results of NENU-9 are summarized in Table S1 (Supporting Information).

CCDC 922227 (for NENU-9) contains the supplementary crystallographic data for this paper. These data can be obtained free of charge from the Cambridge Crystallographic Data Centre via [www.ccdc.cam.ac.uk/data\\_request/cif](http://www.ccdc.cam.ac.uk/data_request/cif).

### Hydrothermal synthesis of NENU-9

Large crystals suitable for single-crystal X-ray determination were synthesized according to the procedure described in the literature.<sup>[9]</sup> A mixture of  $\text{Cu}(\text{NO}_3)_2 \cdot 3\text{H}_2\text{O}$  (0.24 g, 1 mmol) and  $\text{H}_5\text{PV}_2\text{Mo}_{10}\text{O}_{40} \cdot 34.5\text{H}_2\text{O}$  (0.2 g, 0.083 mmol) in distilled water (10 mL) was stirred for 20 min and then  $\text{H}_3\text{BTC}$  (0.21 g, 1 mmol) and  $[(\text{CH}_3)_4\text{N}]\text{OH}$  (0.09 g, 1 mmol) were added successively. The mixture was stirred for 30 min at room temperature. The turbid mixture (pH 2–3) was then sealed in a Teflon-lined autoclave and heated at  $180^\circ\text{C}$  for 24 h, followed by slow cooling to room temperature. Green octahedral crystals were then collected.

### Preparation of phase-pure NENU-9N by the solution method

NENU-9N (average diameter = 1.3  $\mu\text{m}$ ): A solution of  $\text{Cu}(\text{NO}_3)_2 \cdot 3\text{H}_2\text{O}$  (0.24 g, 1 mmol) and  $\text{H}_5\text{PV}_2\text{Mo}_{10}\text{O}_{40} \cdot 34.5\text{H}_2\text{O}$  (0.22 g, 0.092 mmol) in distilled water (10 mL) was stirred for 20 min (solution A). The pH of the solution was adjusted to 2.5 by the dropwise addition of 1 M NaOH.  $\text{H}_3\text{BTC}$  (0.14 g, 0.67 mmol) was dissolved in alcohol

(10 mL), and this solution was added dropwise to solution A with continuous stirring at room temperature. A green precipitate appeared gradually. The precipitate was collected by centrifugation and washed through centrifugation and redispersion with alcohol and distilled water. After drying in an oven at  $60^\circ\text{C}$  for 24 h, the nanocrystalline material with an average diameter of 1.3  $\mu\text{m}$  was obtained.

NENU-9N (average diameter = 550 nm): A solution of  $\text{Cu}(\text{OAc})_2 \cdot \text{H}_2\text{O}$  (0.2 g, 1 mmol) and  $\text{H}_5\text{PV}_2\text{Mo}_{10}\text{O}_{40} \cdot 34.5\text{H}_2\text{O}$  (0.22 g, 0.092 mmol) in distilled water (10 mL) was stirred for 20 min (solution A). The pH of the solution was adjusted to 2.5 by the dropwise addition of 1 M NaOH.  $\text{H}_3\text{BTC}$  (0.14 g, 0.67 mmol) was dissolved in alcohol (10 mL), and this solution was added dropwise to solution A with continuous stirring at room temperature. A green precipitate appeared immediately. The precipitate was collected by centrifugation and washed through centrifugation and redispersion with alcohol and distilled water. After drying in an oven at  $60^\circ\text{C}$  for 24 h, the nanocrystalline material with an average diameter of 550 nm was obtained. The nanocrystals were characterized by FTIR spectroscopy (Figure S16, Supporting Information) and PXRD (Figure S17, Supporting Information).

NENU-9N (average diameter = 80 nm): A solution of  $\text{Cu}(\text{OAc})_2 \cdot \text{H}_2\text{O}$  (0.2 g, 1 mmol) and  $\text{H}_5\text{PV}_2\text{Mo}_{10}\text{O}_{40} \cdot 34.5\text{H}_2\text{O}$  (0.22 g, 0.092 mmol) in distilled water (10 mL) was stirred for 20 min (solution A). The pH of the solution was adjusted to 4.0 by the dropwise addition of 1 M NaOH.  $\text{H}_3\text{BTC}$  (0.14 g, 0.67 mmol) was dissolved in alcohol (10 mL), and this solution was added dropwise to solution A with continuous stirring at room temperature. A green precipitate appeared immediately. The precipitate was collected by centrifugation and washed through centrifugation and redispersion with alcohol and distilled water. After drying in an oven at  $60^\circ\text{C}$  for 24 h, the nanocrystalline material with an average diameter of 80 nm was obtained.

### Preparation of phase-pure NENU-9N by the mechanochemical method

$\text{Cu}(\text{NO}_3)_2 \cdot 3\text{H}_2\text{O}$  (0.24 g, 1 mmol) and  $\text{H}_5\text{PV}_2\text{Mo}_{10}\text{O}_{40} \cdot 34.5\text{H}_2\text{O}$  (0.22 g, 0.092 mmol) were dissolved successively in distilled water (10 mL), and the pH of the solution was adjusted to 2–4 with 1 M NaOH. After evaporating the solvent to dryness, the powder was mixed with  $\text{H}_3\text{BTC}$  (0.14 g, 0.67 mmol) in an agate mortar and grinded for approximately 5 min. The color of the mixture turned green gradually. The product was washed through centrifugation and redispersion with alcohol and distilled water. After drying in an oven at  $60^\circ\text{C}$  for 24 h, phase-pure NENU-9N with an average diameter of approximately 150 nm was obtained (Figure S3, Supporting Information) in approximately 91% yield (calculated on the basis of Cu). FTIR spectroscopy and PXRD demonstrated that the products were phase-pure NENU-9N (Figures S16 and S17, Supporting Information). Copper acetate, copper sulfate, and copper chloride could also be used as copper precursors.

### Catalytic oxidation of DBT to DBTO<sub>2</sub> in decalin

In a typical case, dibenzothiophene (DBT; 0.147 g, 0.8 mmol) was added to decalin (50 mL), and the final sulfur content was approximately 500 ppmw. When the reaction system temperature had stabilized at  $80^\circ\text{C}$ , NENU-9N (0.044 g, 0.01 mmol, average size 550 nm) and isobutyraldehyde (0.72 mL, 8 mmol) were added, and molecular oxygen was bubbled through the reaction solution. The complete reaction was performed with continuous stirring. An ali-

quot of the ration mixture was periodically removed and put into an ice chamber to stop the reaction. The progress of the reaction was analyzed by gas chromatography. Upon completion of the reaction, the catalyst was recovered by centrifugation and washed with distilled water and anhydrous ethanol and then oven dried for reuse. Comparative studies with the use of NENU-9 (0.048 g, 0.01 mmol, average size = 300  $\mu\text{m}$ ) and  $\text{H}_5\text{PV}_2\text{Mo}_{10}\text{O}_{40}\cdot 34.5\text{H}_2\text{O}$  (0.024 g, 0.01 mmol, average size = 300  $\mu\text{m}$ ) as catalysts were performed under otherwise identical conditions.

### Oxidation and desulfurization of prehydrotreated diesel

In a typical case, prehydrotreated diesel (50 mL, sulfur content  $\approx$  500 ppmw) was heated to 80  $^\circ\text{C}$ , NENU-9N (0.044 g, 0.01 mmol, average size 550 nm) and isobutyraldehyde (0.72 mL, 8 mmol) were added, and molecular oxygen was bubbled through the reaction solution. The reaction was stirred continuously for 1.5 h. Then, the sulfones in the oxidized diesel were removed by a polar extractant (for example, acetonitrile or 1-methyl-2-pyrrolidone), and the product was analyzed by gas chromatography.

### Liquid adsorption experiment

DBT (0.147 g, 0.8 mmol) was added to decalin (50 mL), and the final sulfur content was approximately 500 ppmw. NENU-9N (1 g, 0.23 mmol) was added, and the reaction mixture was placed in an oven at 120  $^\circ\text{C}$  for 12 h and stirred continuously. An aliquot of the mixture was periodically removed and analyzed by gas chromatography.

### Catalyst leaching experiment

NENU-9N (0.044 g, 0.01 mmol, average size 550 nm) was soaked in distilled water (50 mL). An aliquot of the solution was removed after 5, 10, 24, and 48 h and analyzed by UV/Vis spectrophotometry.

### Acknowledgements

This work was supported by the National Natural Science Foundation of China (Grants 21171032 and 21231002) and the Open Research Fund of the State Key Laboratory of Inorganic Synthesis and Preparative Chemistry (Jilin University, Grant 2012–10).

**Keywords:** nanocatalysts · desulfurization · metal–organic frameworks · nanostructures · polyoxometalates

- [1] a) T. V. Choudhary, J. Malandra, J. Green, S. Parrott, B. Johnson, *Angew. Chem.* **2006**, *118*, 3377–3381; *Angew. Chem. Int. Ed.* **2006**, *45*, 3299–3303; b) A. Röthlisberger, R. Prins, *J. Catal.* **2005**, *235*, 229–240.
- [2] a) R. T. Yang, A. J. Hernández-Maldonado, F. H. Yang, *Science* **2003**, *301*, 79–81; b) A. J. Hernández-Maldonado, R. T. Yang, *J. Am. Chem. Soc.* **2004**, *126*, 992–993; c) K. A. Cychosz, A. G. Wong-Foy, A. J. Matzger, *J. Am. Chem. Soc.* **2008**, *130*, 6938–6939; d) K. A. Cychosz, A. G. Wong-Foy, A. J. Matzger, *J. Am. Chem. Soc.* **2009**, *131*, 14538–14543.

- [3] B. Y. Zhang, Z. X. Jiang, J. Li, Y. N. Zhang, F. Lin, Y. Liu, C. Li, *J. Catal.* **2012**, *287*, 5–12.
- [4] a) P. Yin, J. Wang, Z. Xiao, P. Wu, Y. Wei, T. Liu, *Chem. Eur. J.* **2012**, *18*, 9174–9178; b) J. H. Xu, S. Zhao, W. Chen, M. Wang, Y. F. Song, *Chem. Eur. J.* **2012**, *18*, 4775–4781; c) J. Zhang, A. J. Wang, X. Li, X. H. Ma, *J. Catal.* **2011**, *279*, 269–275; d) C. Li, Z. Jiang, J. Gao, Y. Yang, S. Wang, F. Tian, F. Sun, X. Sun, P. Ying, C. Han, *Chem. Eur. J.* **2004**, *10*, 2277–2280.
- [5] a) C. Fleming, D. L. Long, N. McMillan, J. Johnston, N. Bovet, V. Dhanak, N. Gadegaard, P. Kogerler, L. Cronin, M. Kadodwala, *Nat. Nanotechnol.* **2008**, *3*, 289–233; b) J. Song, Z. Luo, D. K. Britt, H. Furukawa, O. M. Yaghi, K. I. Hardcastle, C. L. Hill, *J. Am. Chem. Soc.* **2011**, *133*, 16839–16846; c) O. A. Kholdeeva, M. N. Timofeeva, G. M. Maksimov, R. I. Maksimovskaya, W. A. Neiwert, C. L. Hill, *Inorg. Chem.* **2005**, *44*, 666–672; d) H. N. Miras, J. Yan, D. L. Long, L. Cronin, *Chem. Soc. Rev.* **2012**, *41*, 7403–7430; e) D.-L. Long, E. Burkholder, L. Cronin, *Chem. Soc. Rev.* **2007**, *36*, 105–121; f) D. L. Long, R. Tsunashima, L. Cronin, *Angew. Chem.* **2010**, *122*, 1780–1803; *Angew. Chem. Int. Ed.* **2010**, *49*, 1736–1758; g) S.-i. Noro, R. Tsunashima, Y. Kamiya, K. Uemura, H. Kita, L. Cronin, T. Akutagawa, T. Nakamura, *Angew. Chem.* **2009**, *121*, 8859–8862; *Angew. Chem. Int. Ed.* **2009**, *48*, 8703–8706; h) K. Kamata, T. Yamaura, N. Mizuno, *Angew. Chem.* **2012**, *124*, 7387–7390; *Angew. Chem. Int. Ed.* **2012**, *51*, 7275–7278; i) Y. Kikukawa, K. Suzuki, M. Sugawa, T. Hirano, K. Kamata, K. Yamaguchi, N. Mizuno, *Angew. Chem.* **2012**, *124*, 3746–3750; *Angew. Chem. Int. Ed.* **2012**, *51*, 3686–3690; j) K. Suzuki, Y. Kikukawa, S. Uchida, H. Tokoro, K. Imoto, S. Ohkoshi, N. Mizuno, *Angew. Chem.* **2012**, *124*, 1629–1633; *Angew. Chem. Int. Ed.* **2012**, *51*, 1597–1601.
- [6] a) W. Qi, Y. Wang, W. Li, L. Wu, *Chem. Eur. J.* **2010**, *16*, 1068–1078; b) A. Proust, R. Thouvenot, P. Gouzerh, *Chem. Commun.* **2008**, 1837–1852.
- [7] a) A. Nisar, J. Zhuang, X. Wang, *Adv. Mater.* **2011**, *23*, 1130–1135; b) Y. W. Hu, Q. H. He, Z. Zhang, N. D. Ding, B. X. Hu, *Chem. Commun.* **2011**, 47, 12194–12196; c) H. Lu, J. Gao, Z. Jiang, Y. Yang, B. Song, C. Li, *Chem. Commun.* **2007**, 150–152.
- [8] a) H. X. Deng, C. J. Doonan, H. Furukawa, R. B. Ferreira, J. Towne, C. B. Knobler, B. Wang, O. M. Yaghi, *Science* **2010**, *327*, 846–850; b) F. Stallmach, S. Groger, V. Kunzel, J. Karger, O. M. Yaghi, M. Hesse, U. Muller, *Angew. Chem.* **2006**, *118*, 2177–2181; *Angew. Chem. Int. Ed.* **2006**, *45*, 2123–2126; c) J. R. Long, O. M. Yaghi, *Chem. Soc. Rev.* **2009**, *38*, 1213–1214; d) H. K. Chae, D. Y. Siberio-Perez, J. Kim, Y. Go, M. Eddaoudi, A. J. Matzger, M. O’Keeffe, O. M. Yaghi, *Nature* **2004**, *427*, 523–527; e) S. M. F. L. Stephen, S. Y. Chui, J. P. H. Charmant, A. G. Orpen, I. D. Williams, *Science* **1999**, *283*, 1148–1150.
- [9] C. Y. Sun, S. X. Liu, D. D. Liang, K. Z. Shao, Y. H. Ren, Z. M. Su, *J. Am. Chem. Soc.* **2009**, *131*, 1883–1888.
- [10] a) X. Wang, J. Zhuang, Q. Peng, Y. Li, *Nature* **2005**, *437*, 121–124; b) S. p. Diring, S. Furukawa, Y. Takashima, T. Tsuruoka, S. Kitagawa, *Chem. Mater.* **2010**, *22*, 4531–4538; c) L. H. Wee, S. R. Bajpe, N. Janssens, I. Hermans, K. Houthoofd, C. E. Kirschhock, J. A. Martens, *Chem. Commun.* **2010**, 46, 8186–8188.
- [11] S. R. Bajpe, C. E. Kirschhock, A. Aerts, E. Breyneert, G. Absillis, T. N. Pa rac-Vogt, L. Giebel, J. A. Martens, *Chem. Eur. J.* **2010**, *16*, 3926–3932.
- [12] O. Shekhah, H. Wang, D. Zacher, R. A. Fischer, C. Wöll, *Angew. Chem.* **2009**, *121*, 5138–5142; *Angew. Chem. Int. Ed.* **2009**, *48*, 5038–5041.
- [13] D. D. Liang, S. X. Liu, F. J. Ma, F. Wei, Y. G. Chen, *Adv. Synth. Catal.* **2011**, *353*, 733–742.
- [14] a) A. M. Khenkin, A. Rosenberger, R. Neumann, *J. Catal.* **1999**, *182*, 82–91; b) M. Hamamoto, K. Nakayama, Y. Nishiyama, Y. Ishii, *J. Org. Chem.* **1993**, *58*, 6421–6425.
- [15] H. Y. Lu, J. B. Gao, Z. X. Jiang, F. Jing, Y. X. Yano, G. Wang, C. Li, *J. Catal.* **2006**, *239*, 369–375.
- [16] G. A. Tsigdinos, C. J. Hallada, *Inorg. Chem.* **1968**, *7*, 437–441.

Received: May 17, 2013

Published online on July 10, 2013